Meteorol Atmos Phys 94, 115–128 (2006)
DOI 10.1007/s00703-005-0174-3

Meteorology and Atmospheric Physics

Printed in Austria

[1] Departamento de Ciências Atmosféricas, Universidade Federal de Campina Grande (UFCG), Brazil
[2] Departamento de Ciências Atmosféricas, Universidade de São Paolo (USP), São Paolo, Brazil

Soil occupation and atmospheric variations over Sobradinho Lake area. Part two: a regional modeling study

M. F. Correia[1], **M. A. F. da Silva Dias**[2], and **M. R. da Silva Aragão**[1]

With 11 Figures

Received April 21, 2005; accepted November 21, 2005
Published online: June 20, 2006

Summary

The impact of the changes on soil cover and land use brought about by the construction of the Sobradinho Dam in the semi-arid region of the São Francisco River Hydrographic Basin is analyzed by means of a numerical model RAMS. Disregarding the influence of a large scale flow, a set of factors were responsible for the creation of a rather complex circulation system that includes mountain-valley winds, lake breeze (LB) and non-conventional circulation all induced by the surface non-homogeneous aspect. Results have demonstrated that the implementation of works of such magnitude brings about environmental changes in an area that stretches far beyond the surroundings of the reservoir. The soil cover alterations due to the ever increasing development of the area with the presence of irrigated crops in a sparsely vegetated region (*caatinga*) does affect land surface characteristics, occasioning for that matter the splitting of the available energy into latent and sensible heat fluxes. LB behavior varies in accordance with atmospheric conditions and also in view of the type of vegetation found in the lake surrounding areas. Hydro availability in root zones, even under adverse atmospheric conditions (high temperature and low air humidity) brings up the high rates of evaporation and plant transpiration that contribute towards the increase of humidity and the fall of temperature in lower atmospheric layers.

1. Introduction

The waters of the São Francisco River are mainly used for electrical power generation. According to IBGE (The Brazilian Institute of Geography and Statistics) data, the construction of the Sobradinho Dam boosted up the use of land, leading to a substantial increment of irrigated farming, whose growth reflects on the utilization of the waters and soil surface features as well as on soil management as a result of replacing native vegetation (*caatinga*) by farming lands. In a semi-arid area, any alteration on the vegetation cover will bring about substantial changes in the atmospheric boundary layer (ABL) structure.

Results of statistical analysis, presented in part I of this paper, confirm that the dam construction has altered the local environment, and that wind and humidity are the most affected meteorological elements. It is the purpose of this work to elucidate the various processes responsible for the behavior of these elements by means of numerical simulations performed with the RAMS model (Regional Atmospheric Modeling System). The model makes it possible to simulate the atmospheric behavior with and without the lake (WL and NL), and evaluate the reservoir impact through the difference between the results obtained from both simulations. The influence of increasing irrigated area was measured by considering the difference between simulations with irrigated crops (WIC) and without irrigated crops (NIC).

The 4a-RAMS model version was used. This model has been extensively used to simulate mesoscale processes that have been validated by case studies (Pielke et al, 1992; Avissar and Pan, 2000; Correia and Silva Dias, 2003). In the present work, both the dimension and location of the main public irrigation perimeters were introduced in the model with considerable precision along with vertical profiles of soil humidity, rendering possible the simulation of water extraction from the roots and its transfer to the atmosphere.

1.1 Native vegetation characteristics

The *caatinga* is the typical vegetation found in regions subjected to long dry periods. The *caatinga* lies in an area that corresponds to about 11% of the Brazilian territory, encompassing most of the northeastern semi-arid region. It is made up of a vegetation complex including deciduous (plants whose leaves fall at certain periods of the year) and xerophilous (plants that possess anatomical and physiological characteristics capable of restricting transpiration) vegetation complex made up of firewood vegetation and a myriad of cacti and bromeliacease.

During long dry periods, the trees are deprived of their leaves, and the soil in between them is left almost without grass or weeds (Fig. 1a). Leaf falling in the absence of rain is seen as one of the flora defense mechanisms to cope with hydro scarcity. However, at the beginning of the rainy season, the vegetation turns green, changing the landscape radically (Fig. 1b). The *caatinga* plants have developed physiological mechanisms that account for the accumulation of nutrients and water storage (roots, and certain types of stem) as a way of getting adapted to the

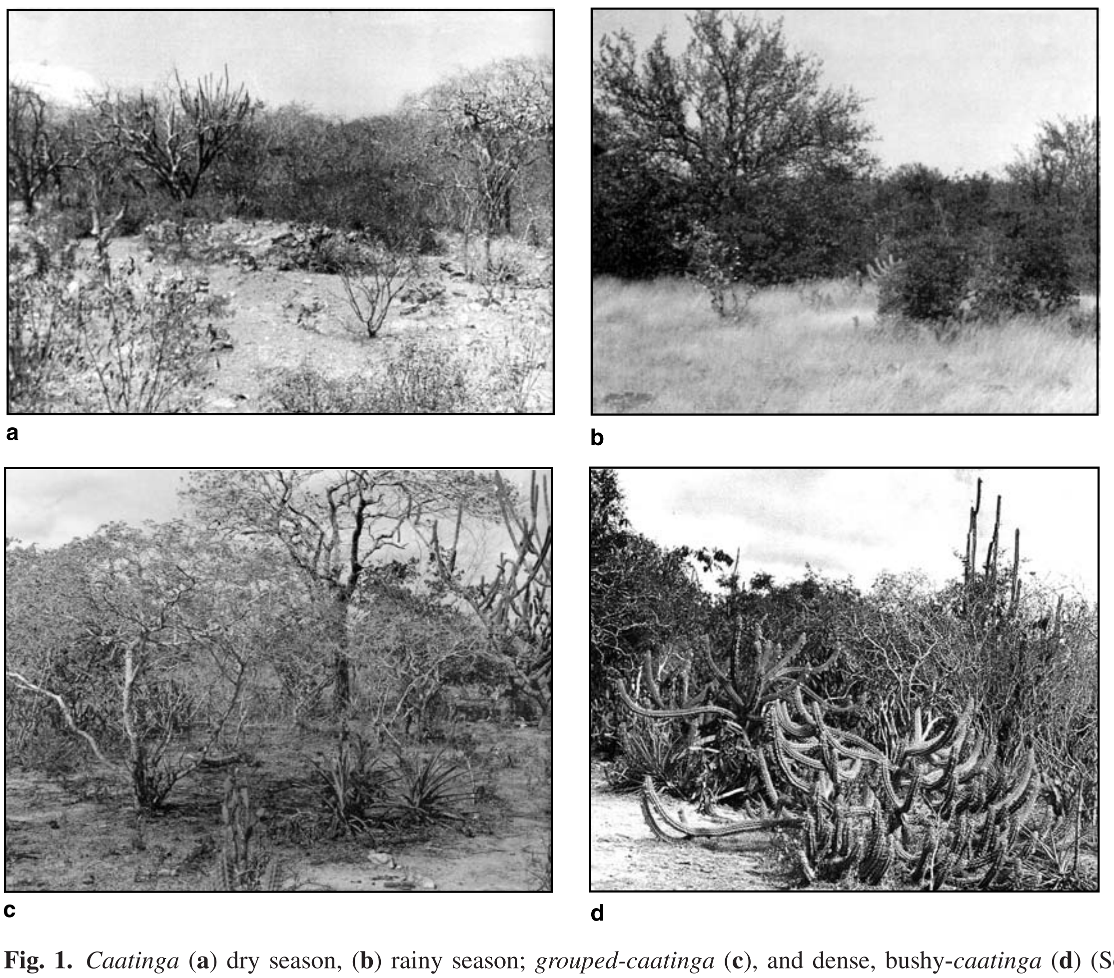

Fig. 1. *Caatinga* (**a**) dry season, (**b**) rainy season; *grouped-caatinga* (**c**), and dense, bushy-*caatinga* (**d**) (Source: Romariz, 1996)

caatinga's dry climate. These are processes that enable the plants to survive the dry season. Taking humidity into account, the *caatinga* vegetation is classified in two groups, each one representing a different kind of landscape: the *agreste* (dry area in northeast Brazil), found in regions closer to the sea, and, therefore, presenting higher humidity in deep soils with taller and denser vegetation; and the *sertão* (the arid and remote interior) to be found deeper in the interior with lower humidity in shallow and rocky terrain.

The so-called *grouped-caatinga* exhibits the kind of vegetation commonly found on the banks of the São Francisco River where the topography presents itself as rugged with elevations not greater than 300 meters. There one can find cacti, bromeliacease and twiggy shrubs; all spread in thickets, easily exposed to the sun rays, with clear areas in between them. The plants are 2–3 meters high, forming a thorny entanglement of vegetation (Fig. 1c). Another kind of vegetation, frequently found in the region, is the dense, bushy *caatinga* which forms a far more compact thorny entanglement. The bushy *caatinga* is thick, but it does not cover the soil completely. The higher specimens reach 5 to 6 meters. Cacti and bromeliacease can also be found in this area (Fig. 1d).

2. Methodology

2.1 Numerical model description

RAMS numerical model evolved from a mesoscale model (Pielke, 1974) and from a cloud model (Tripoli and Cotton, 1982). This model is a rather versatile numerical code whose structure allows simulations with several degrees of complexity. RAMS is a non-hydrostatic, three dimensional model with a vertical coordinate that follows the topography. It also includes surface physical processes through a soil layer and a surface layer with vegetation, turbulent processes, cumulus convection and cloud microphysical processes parameterizations, short and long wave radiation. This model is made up of an atmospheric and a surface module that interact with each other, given the appropriate boundary conditions. The heat and humidity fluxes parameterization scheme inside the bared soil was developed by Tremback and Kessler (1985) based on a multi-layer model put forward by Mahrer and Pielke (1977), and MacCumber and Pielke (1981). The prognostic temperature and soil wetness equations have been derived from the diffusion equation that has been explicitly solved. Details of the model's equations and structure may be found in Avissar and Pielke (1989) and Pielke et al (1992).

There exists a direct link between the weather conditions in the sub-medium São Francisco River and the surface wind behavior (Silva Aragão et al, 1997). Months with below normal rainfall are characterized by winds associated with the South Atlantic subtropical anticyclone (east/southeast trade winds), whereas months with above normal rainfall exhibit other directions due to the influence of other atmospheric systems such as the Intertropical Convergence Zone (ITCZ), Upper Tropospheric Cyclonic Vortices and Frontal Systems coming from southern Brazil. In a favorable synoptic situation, mechanical and thermodynamical effects of the topography upon the atmospheric flow may contribute towards an intensification of mountain-valley winds or give rise to specific systems resulting from scale interaction.

Under such a context, upper air data from two radiosondes launched in Petrolina-PE during the region's dry season were selected to represent contrasting situations in terms of the mean wind and moisture content. The June 5th, 1985 sounding (ATM85) – a typical situation in which one can notice the weakening of the southeasterly trade winds due to the penetration of a frontal origin system (Silva Aragão et al, 2000) that altered the region's weather conditions thoroughly.

The September 30th, 1999 sounding (ATM99) describes a convectively stable atmosphere with a typical synoptic environment of Petrolina, almost always under the influence of the South Atlantic subtropical high. On this day, surface wind at the time of observation was coming from the east with an intensity of $6\,\mathrm{ms}^{-1}$, close to the monthly mean of $4–5\,\mathrm{ms}^{-1}$ as obtained by Correia (2000).

Aiming at doing away with the influence of the mean wind and highlighting the surface forcing effects, the wind of the soundings was not taken into account. The influence of the surface forcings is isolated, considering the clear sky meteorological situation in complex terrain. Clear sky condition is secured by keeping the model's microphysical scheme deactivated and by using the radiation parameterization suggested by Mahrer and Pielke (1977). Such parameterization allows one to calculate the surface short wave and long wave radiation fluxes, without considering the liquid and solid phases of atmospheric water; only water vapor is considered.

In the case of ATM99, the error on deactivating the model microphysical processes may be considered to be negligible in view of the small incidence of clouds on that day. In the case of ATM85, an increase in cloudiness in the afternoon endangered somehow the results due to the elimination of the cloudiness influence on the surface energy balance.

Each model integration lasted for 24 hours and started at 03:00 LT (local time) with a homogeneous structure obtained by extending the sounding data to the entire domain. A vertical grid was built up for 30 levels with 50-meter initial Δz, increasing upward the 1.2 ratio up to 1 km. From this level upwards, the Δz was constant up to the top of the model.

2.1.1 The lake impact

Two grids with spatial resolution of six and two kilometers – grids 1 and 2 respectively, both centered in Petrolina-PE (9.4° S–40.5° W) have been used. Grid 1 covers an area of approximately $562 \times 562\,\text{km}^2$, and grid 2, an area of $184 \times 184\,\text{km}^2$. Specification of the topography and soil occupation, including the vegetation type and the location and dimension of the Sobradinho reservoir, was based on RAMS data files (1 km resolution) obtained by means of advanced very high resolution radiometers (AVHRR). As displayed by these files, the vegetation cover is predominantly of the types *temporary bush* and *semi-desert*. In both northwest and southwest domain sectors, close to the lake, there exist large vegetated areas. The type of soil used in the simulations was the sandy clay loam. The soil wetness profile was considered uniform within the domain, and the choice of a constant 0.40 of the saturation value was based on the model sensitivity results. Regrettably, this parameter is not systematically observed in the region, unless for very specific purposes. This is a variable that has a significant impact on the local circulation simulations. A too high value can diminish the thermal contrast between the lake surface and its surrounding area, reducing the lake's breeze intensity. On the other hand, a too low value can create excessively intense circulations and produce unrealistic results.

The changes brought about by the dam construction have been assessed by means of simulations with lake (WL) and without lake (NL). Considering the fact that for these experiments the lake itself represents the forcing mechanism, data files have been created so as to do away with the flooded area within the domain. The analyses were based upon the ATM85 and ATM99 experiments.

2.1.2 The impact of changes on soil use

Specification of the soil occupation including the irrigation perimeters required to insert these areas into the numerical domain. For that matter, a map developed by the Departamento Nacional de Obras Contra as Secas (National Department Against Droughts) providing information on the Northeast semi-arid region water resources was used. By superimposing grids with $2 \times 2\,\text{km}^2$, it was possible to determine accurately the dimension and location of the main public irrigation perimeters in operation, and also to define the number of grid points that would correspond to all vegetation groups. Figure 2 shows the numerical domain covered by grid 2, together with the Sobradinho Lake and irrigated areas. The soil used in the simulations is of the type *Sandy clay loam*, and it is simulated for an underground depth of 1.0 m, represented in the model by 10 levels with higher resolution close to the surface, and progressively lower resolution with depth. The hydraulic properties of this soil are found in MacCumber and Pielke (1981), and Tremback and Kessler (1985).

2.1.3 Soil wetness effect

Segal et al (1988) have demonstrated that the soil should be initialized with a drier profile close to the surface and a damper profile at the depth of the roots as long as one's objective is to represent the impact of stress-free vegetated areas on mesoscale atmospheric circulations. Aiming at assess-

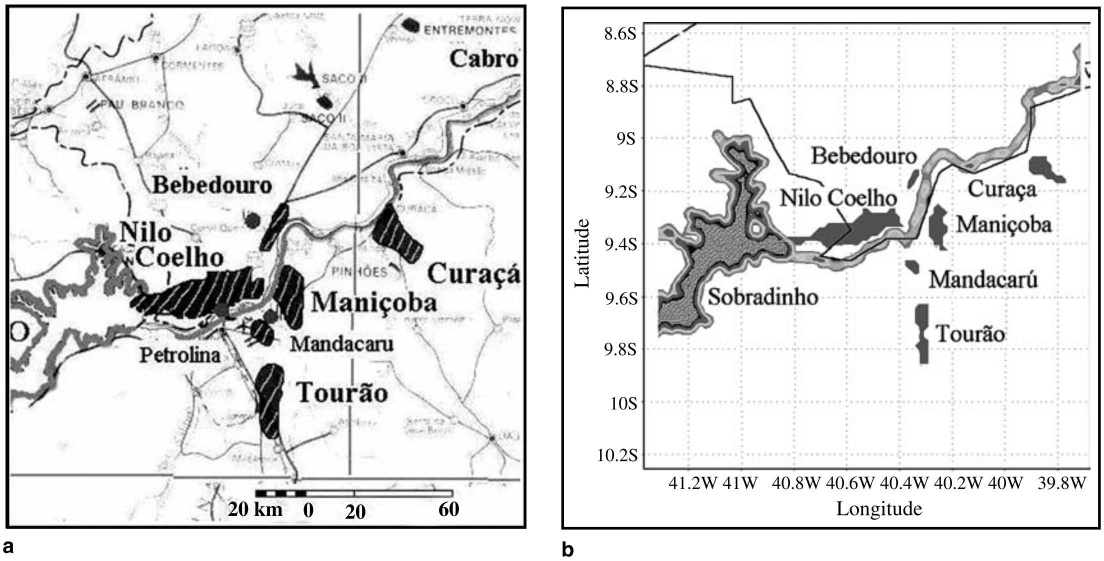

Fig. 2. Map showing the localization of the Sobradinho Lake and the main public irrigation perimeters in the sub-medium São Francisco River (**a**), and the numerical domain covered by grid 2 (**b**)

Table 1. Initial conditions and properties of the soil used in the ATM99 simulations (IC: irrigated crop, SD: semi-desert vegetation; type of soil: sandy clay loam)

Soil depth (m)	Moisture content of the soil	
	IC	SD
−0.02	0.60	0.17
−0.05	0.60	0.17
−0.10	0.60	0.17
−0.20	0.60	0.17
−0.35	0.60	0.17
−0.45	0.80	0.20
−0.50	0.80	0.20
−0.60	0.80	0.20
−0.80	0.80	0.20
−1.00	0.80	0.20

ing the impact of replacing the *caatinga* by irrigated crops, the model was initialized with a soil wetness profile and structure as shown on Table 1. Analyses were based on experiments carried out with ATM99.

The SD vegetation was selected as the predominant type in the domain under investigation. Some parameters which are demonstrative of this type of vegetation have been altered so as to better represent the values found in the area of study under environmental conditions most typical of the dry season.

The vegetation cover fraction of the *caatinga* region is above the value of 0.10 (typical of desert areas), as defined in the model scheme, throughout the dry season. During this period most plants' leaves fall as a defense mechanism against water scarcity. Equally important is the way some branches and twigs get all entangled to form a bushy protection against direct solar incidence, preserving the soil humidity for a much longer period. This effect, which somehow produces larger shadowy areas, was responsible for an increase in soil cover fraction that jumped from 0.10 to 0.30.

Another very important feature concerning the physical processes discussed in this paper is the distribution and percentage of roots in the soil's upper layer. This represents a most significant vegetation morphological aspect as found in the semi-arid and consequently must be treated as adequately as possible. This parameter, which represents the water percentage extracted from the soil upper layer through the transpiration process has a value of 0.80 in the model, being as it is unrealistic for the region under analysis. The *caatinga* vegetation species possess deep roots which have in some regions ramifications on the soil's upper layers so as to capture as much water as possible during the rainy season. Nevertheless, it is also natural to find areas where roots go deeper into the soil in search of water. Excavations carried out in the semi-arid have shown the existence of underground water at a depth of 5 to 36 meters, though this is not common in the area (Rizzini, 1997). This was taken into account by replacing the value of 0.80 by 0.50.

3. Results and discussion

3.1 Lake effect

Figure 3 shows the horizontal wind fields obtained in the simulations with lake (WL) and without lake (NL), and their difference at 15:00 LT for ATM85 and ATM99 on grid 2 domain.

A comparison between the WL and NL simulation results reveals similar configurations for both cases. The flow suggests that the topographic factor is dominant on the intensity and direction of thermally forced winds. Local circulations are basically controlled by anabatic winds on the slopes of higher areas within the lake region. On the other hand, the pressure gradient resulting from the difference between air temperature above the water and over the surrounding areas gives rise to yet another thermally forced circulation known as lake breeze (LB). However, the direction and intensity of the flow can be influenced by the topography, the lake bank configuration, the surrounding vegetation type and the atmospheric thermodynamic structure.

Figure 3e and f illustrates the specific contribution of the presence of the lake upon the local circulation by the wind field resulting from the difference between both simulations. The effects are far more evident in ATM85.

The difference field between the two simulations for ATM99 shows that the lake contributed slightly for the thermally induced flow. This LB behavior results from the influence of the atmospheric thermodynamic characteristics, the lake neighboring type of vegetation and the area topography.

In ATM99, the anabatic winds at 15:00 LT are visibly contrary to the LB penetration. In ATM85 this effect cannot be noticed, and the LB is seen to expand eastwards. The difference between the anabatic winds as observed in both simulations, from which the ATM99 is seen as having produced far more intense values, is directly dependent on the atmospheric features, since the soil cover and the topography are identical in both cases. In situations with relatively low humidity content, the surface evaporation rate is initially high. Most of the energy absorbed by the surface is redistributed by latent heat flux. In time, a gradual drying up of the soil's upper layers can be noticed; evaporation decreases and temperature reaches higher values. Strong thermal gradients are created as a result of the different altitudes and terrain inclinations.

The redistribution of energy absorbed at the surface through sensible (H) and latent heat fluxes (LE) is a result of the vegetated soil main features. According to Pielke et al (1992) the intensity of thermally induced circulations is directly related to the magnitude and horizontal distribution of the surface heat fluxes. Consequently, LB behavior can be altered in the presence of vegetation in the vicinities of the lake.

Plant transpiration rate is also affected by the atmospheric humidity content, and, considering the type of vegetation, there exists a major or minor stomatic resistance affecting the spatial distribution of the surface energy fluxes.

In situations when the plants transpire effectively, the energy absorbed at the surface is mostly redistributed through latent heat flux. The opposite can be seen in regions with bare soil or soil covered with stressed vegetation, since the energy is basically redistributed as sensible heat. The plant' stomas govern Bowen's ratio on vegetated surfaces (Avissar and Pielke, 1989).

Figure 4 shows the horizontal distribution of the sensible heat flux (H) in grid 2 domain for ATM85 and ATM99. One can see that, for the same conditions of soil humidity and vegetation cover, the spatial distribution of H changes when the atmospheric thermodynamic properties are modified.

Figure 5 shows the wind field obtained as a result of the difference between the WL and NL simulations for ATM85 in grid 1 domain (6 km resolution). The whole area affected by the LB is well defined and clearly seen at 15:00 LT (Fig. 5a). However, at 18:00 LT (Fig. 5b), a weakening of LB circulation can be noticed to the south of the lake, caused by catabatic winds created by the mountain slopes' radiative cooling. On the opposite side of the lake, where the ground is flat, and there occurs a reduction on turbulent fluxes, the lake's impact is far more noticeable.

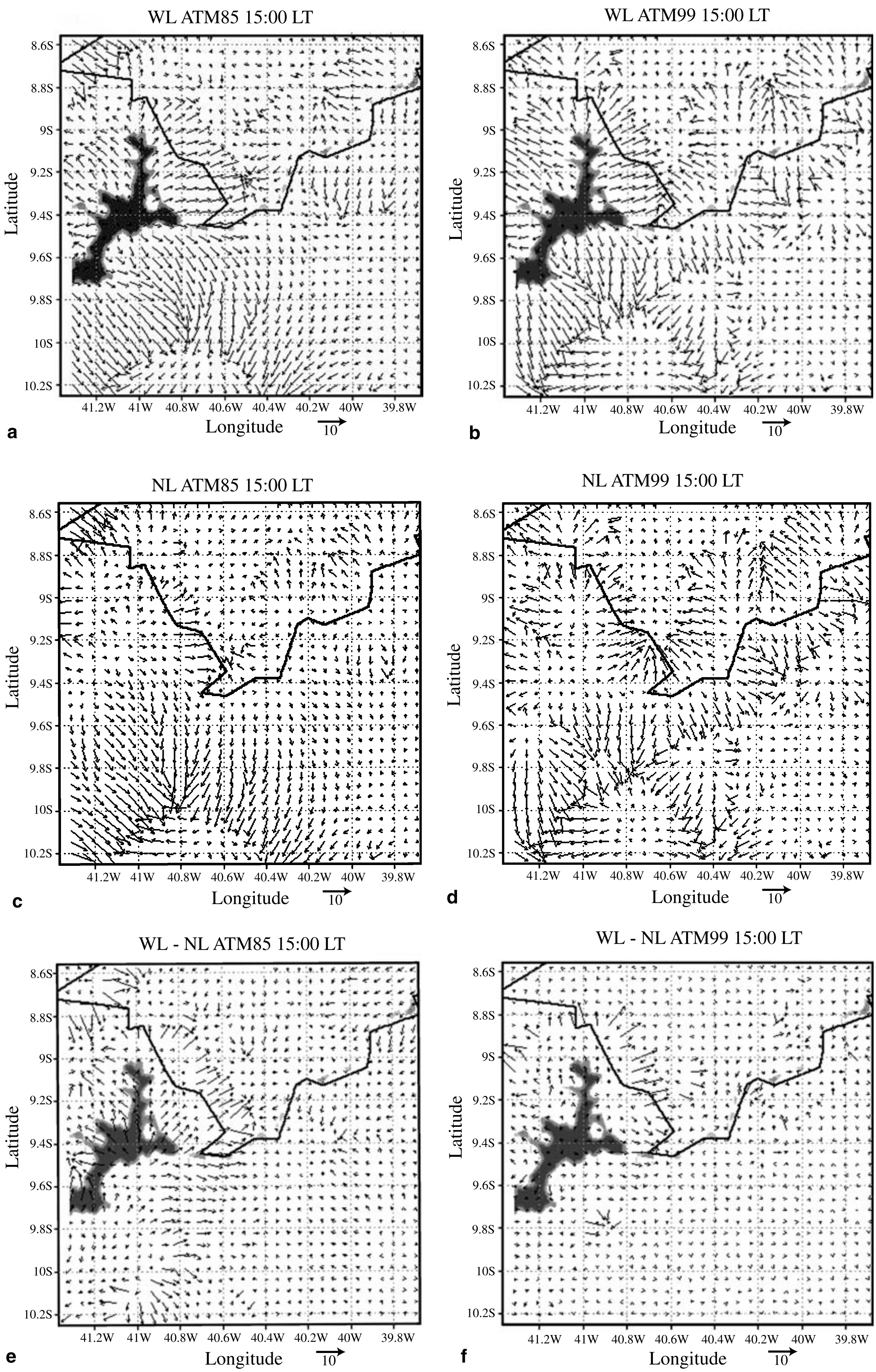

Fig. 3. Wind field (ms^{-1}) at 24 meters above the surface at 15:00 LT on grid 2 domain (2 km resolution) for ATM85 and ATM99. The gray areas represent the Sobradinho Lake and the São Francisco River. Wind scale can be found below each illustration

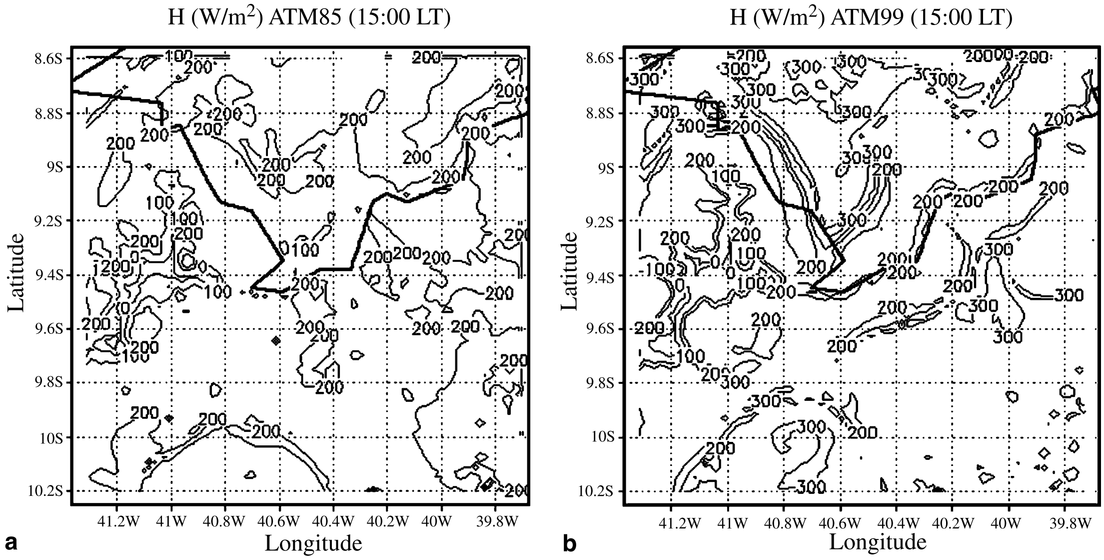

Fig. 4. Sensible heat flux horizontal distribution (Wm^{-2}) in grid 2 domain (2 km resolution) for: (**a**) ATM85, and (**b**) ATM99

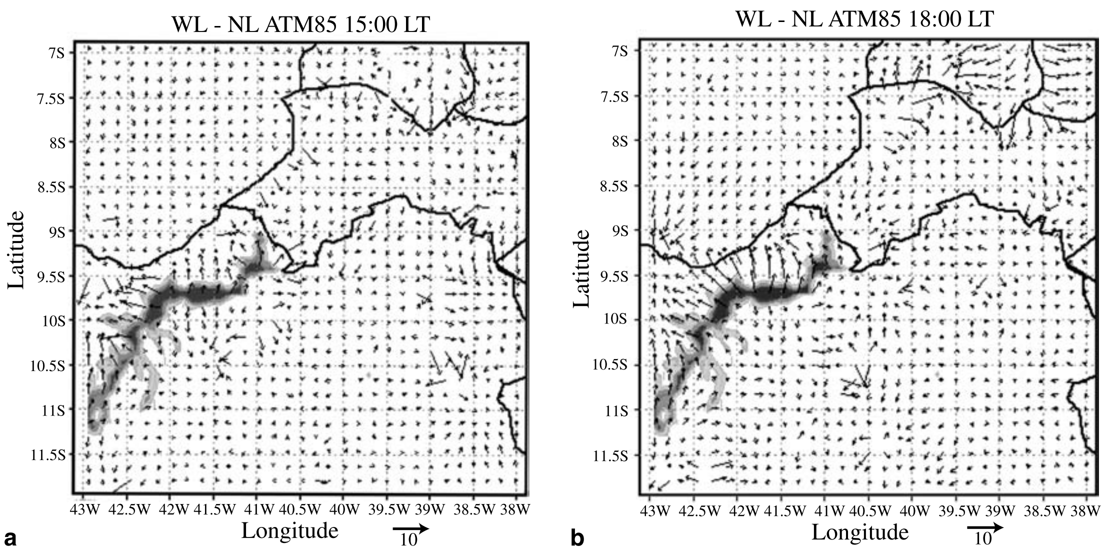

Fig. 5. Difference wind fields (ms^{-1}) between the simulations with lake (WL) and without lake (NL) in grid 1 domain (6 km resolution) at 24 m above the surface for ATM85: (**a**) 15:00 LT and (**b**) 18:00 LT. The gray area represents the Sobradinho Lake

3.1.1 Air temperature and humidity

Figure 6 shows air temperature and mixing ratio fields resulting from the difference between the WL and NL simulations. One can see that there occur a temperature reduction and an increase in atmospheric humidity specially in the area affected by the LB. It has become apparent, as one can see from the illustrations of both ATM85 and ATM99, that the region to the east of the 40.5° W meridian, where the stations of Petrolina, Bebedouro and Mandacaru are located, was only slightly affected by the lake.

3.2 Soil humidity effect

The main purpose of these analyses is to assess the atmospheric response to the inclusion of irrigated crops in areas that are covered with scanty vegetation as the SD type, and also to estimate the influence of such discontinuity in vegetation cover on the genesis of thermally induced circulations.

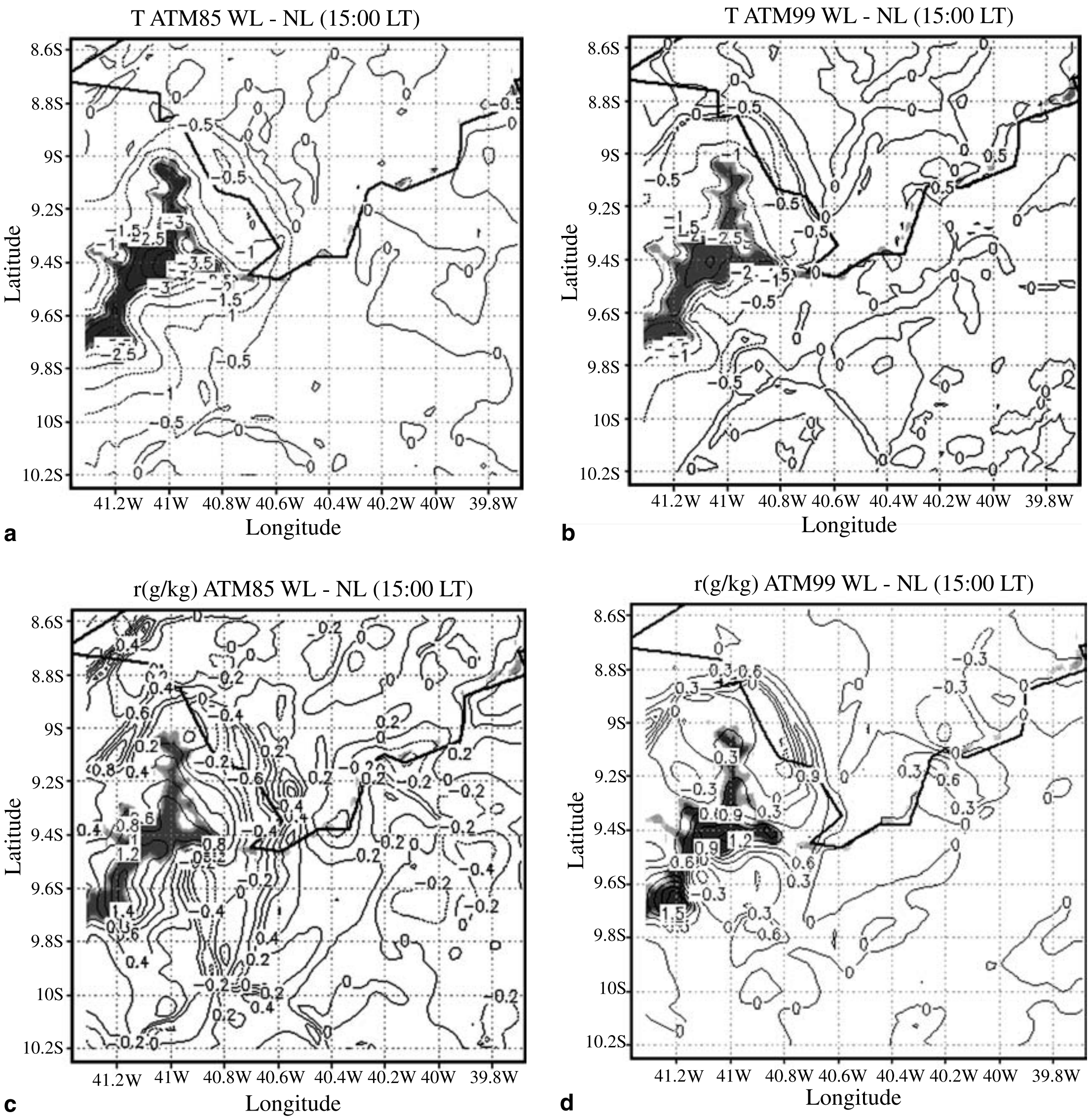

Fig. 6. Difference air temperature (°C) and mixing ratio ($g\,kg^{-1}$) fields between the WL and NL simulations at 24 m above the surface at 15:00 LT for: (**a**) and (**c**) ATM85; (**b**) and (**d**) ATM99

3.2.1 Wind, latent heat and sensible heat

Figure 7 shows wind, latent (LE) and sensible (H) heat fluxes fields resulting from the difference between the WIC and NIC simulations at 12:00 and 15:00 LT for ATM99. The H differences between the irrigated crops (WIC) and semi-desert (NIC) areas are far more noticeable at 15:00 LT.

A significant factor leading to the results from the irrigated areas is the ATM99 low atmospheric humidity content that, in conjunction with the higher air temperature, intensify the soil evaporation process, enhancing surface drying up, greater warming up and increase of H values which is rendered more evident at 12:00 LT.

Another interesting aspect can be noticed in the wind field. The divergence of the flow over the irrigation perimeters is noticeable, especially at 15:00 LT. Discontinuity in vegetation cover between the regions with SD and IC can also be associated with horizontal gradients of albedo and soil humidity, and, as a result, with horizontal gradients of H. These, by their turn, are responsible for the induction of thermally direct circulations in the IC areas best known as non-classical mesoscale circulations. The flow near the surface goes from the relatively cool air areas (IC) towards warmer air areas (SD).

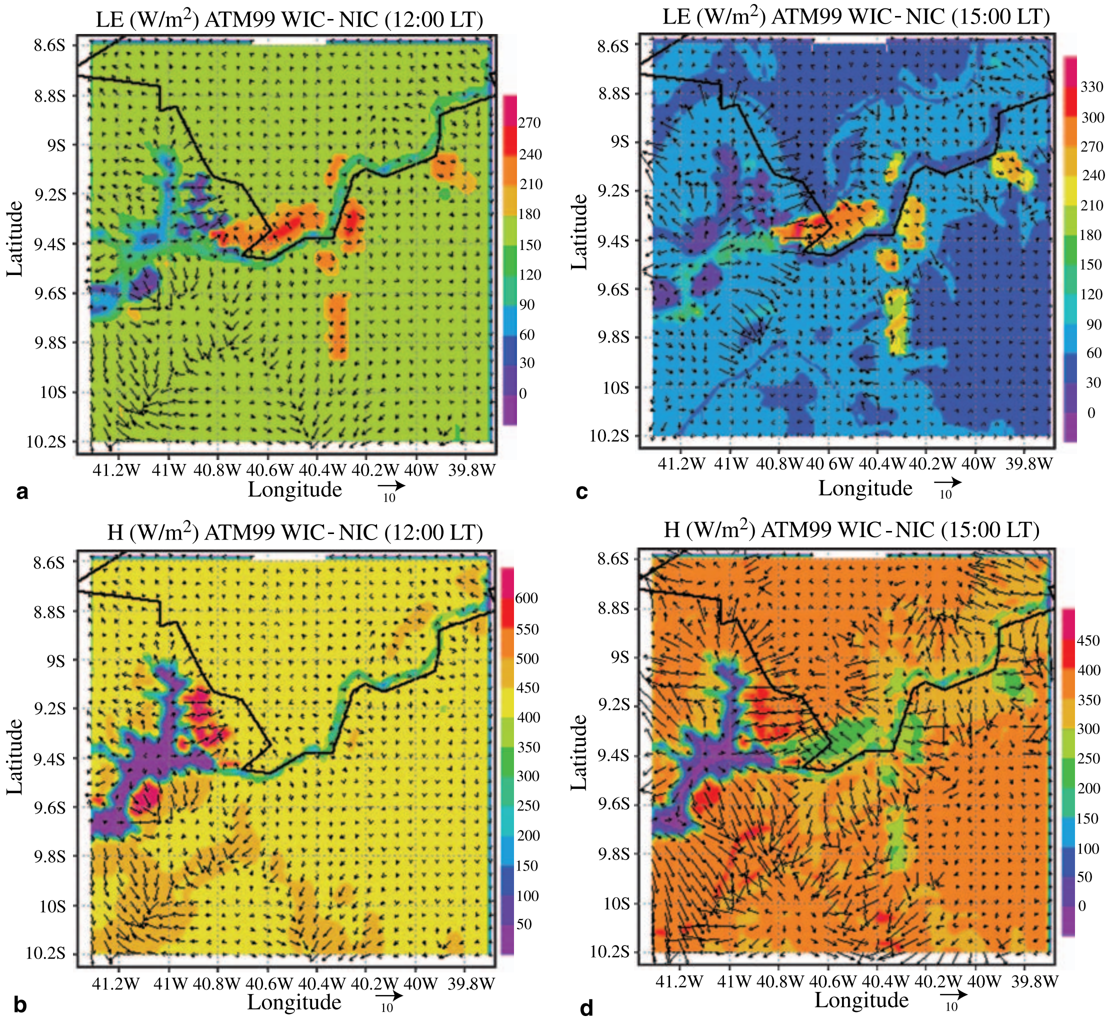

Fig. 7. Difference wind (ms^{-1}), latent (LE) and sensible (H) heat fluxes (Wm^{-2}) fields between the WIC and NIC simulations for ATM99 with irrigated crops (IC) and semi-desert (SD) for: (**a**) and (**b**) 12:00 LT; (**c**) and (**d**) 15:00 LT. The scales used for the heat fluxes and wind vector are seen at the side and below each panel, respectively

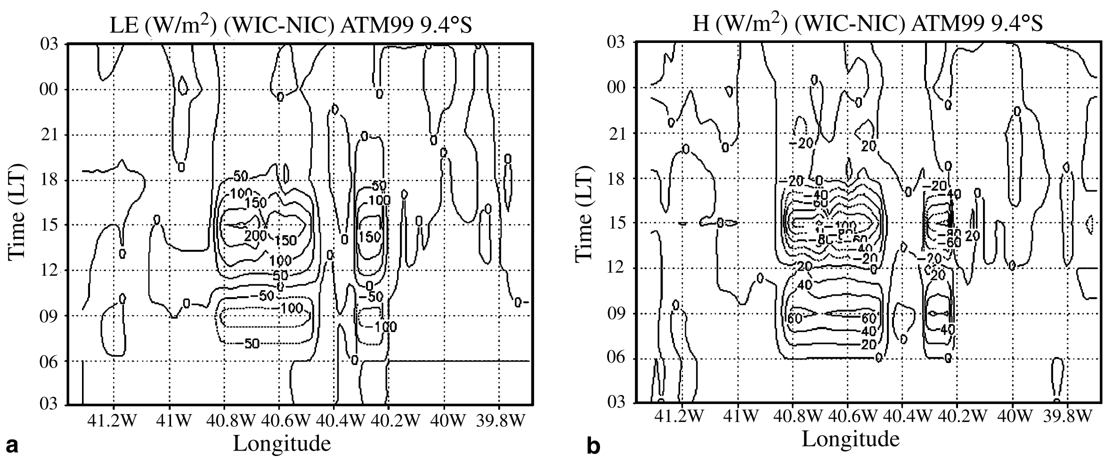

Fig. 8. Daily evolution of the (**a**) latent (LE) and (**b**) sensible (H) heat fluxes (Wm^{-2}) at 9.4° S for ATM99, resulting from the difference between the WIC and NIC simulations

The effect of irrigation on the daily evolution of surface fluxes, as obtained from the difference between simulations with irrigated crops and non-irrigated crops (WIC-NIC) is shown in Fig. 8. Such results demonstrate a great atmospheric sensitivity to the inclusion of IC in an area of scanty vegetation. The radiation quantity that is absorbed at the surface increases as a result of a lower albedo. The soil water availability is crucial to a higher LE and the consequent reduction of H. The water extraction from the soil through the roots represents one of the main mechanisms responsible for this behavior.

Vertical cross sections of the zonal wind component at 12:00 and 15:00 LT, at 9.4° S, obtained in the WIC simulation and from the difference between the WIC and NIC simulations are shown in Fig. 9. The effect of irrigation on the genesis of a breeze-like circulation is evident in Fig. 9b–d. The circulation intensity reaches values of about 2 ms^{-1} at 15:00 LT.

3.2.2 Air temperature and humidity

The difference between the simulations carried out with irrigated crops (WIC) and without irrigated crops (NIC) reveals a fall in the values of

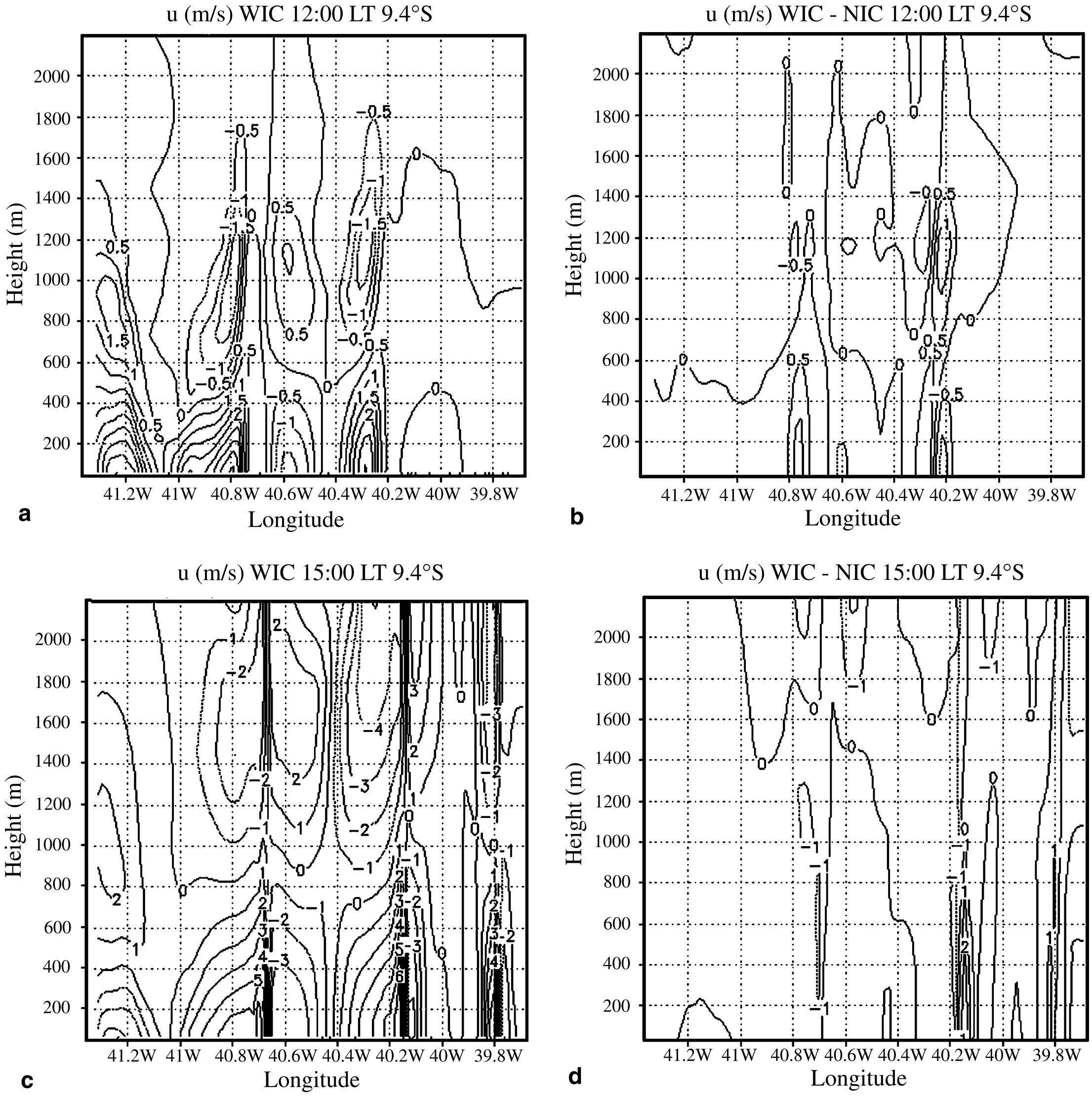

Fig. 9. Vertical cross section of the zonal wind component at 9.4° S for ATM99 obtained from the simulation with irrigated crops (WIC) and resulting from the difference between the simulations with irrigated crops (WIC) and non-irrigated crops (NIC) for: (**a**) and (**b**) 12:00 LT; (**c**) and (**d**) 15:00 LT

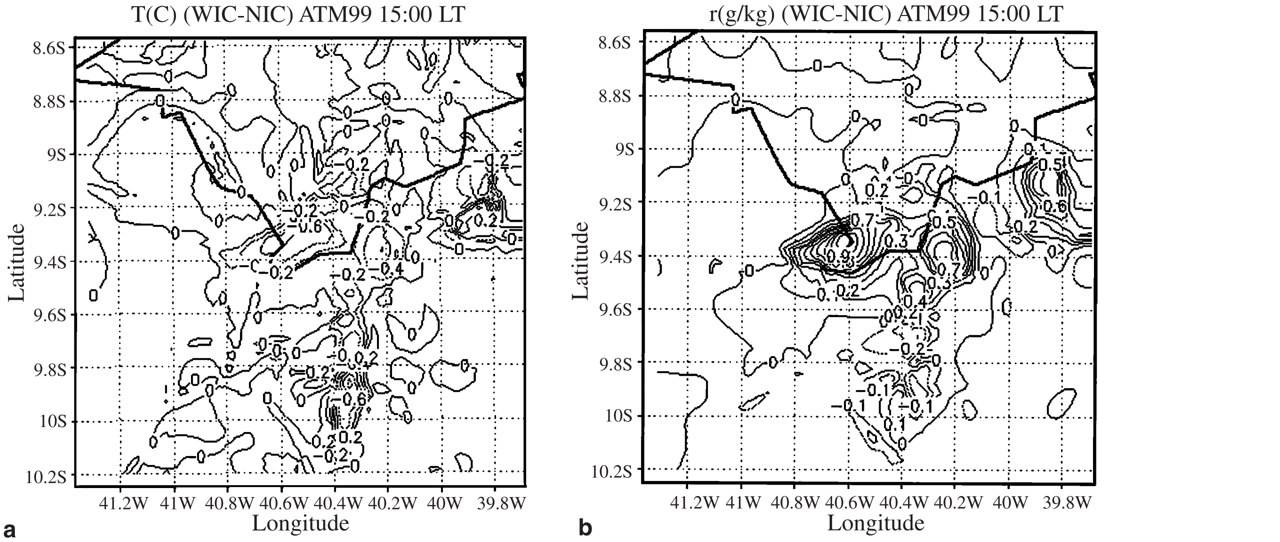

Fig. 10a. Air temperature (°C) and (**b**) mixing ratio ($g\,kg^{-1}$) fields at 24 m above the surface at 15:00 LT for ATM99, resulting from the difference between the simulations with irrigated crops and without irrigated crops (WIC-NIC)

this variable where the irrigation perimeters are to be found as shown in Fig. 10a. The fall in air temperature in the area of the Nilo Coelho irrigation perimeter area comes to 0.7 °C. Analogous to the air temperature, the increase in the mixing ratio becomes evident in the irrigation perimeter (Fig. 10b). Unlike the results obtained in the experiments carried out to verify the lake impact upon these climatic elements, the area affected by irrigation coincides exactly with the region where the stations of Petrolina, Bebedouro and Mandacaru are located.

It is unquestionable that the degree of influence that irrigation exerts on atmospheric humidity depends on the area dimension and on environmental conditions. The highest values are found in the region of the Nilo Coelho Perimeter. In the Bebedouro area, the relatively low increase goes against the observational analysis results that point towards significant changes in that region. Such an apparent contradiction comes as a result of the horizontal grid resolution used in the numerical experiments. Though convenient for identifying the relation between the irrigation process and the increase in atmospheric humidity, that grid is not adequate for revealing the real impact of the Bebedouro perimeter.

Another apparent contradiction between the observational and numerical results lies in the enhancement of this variable in the region of Petrolina (9.4° S–40.5° W) where no statistically significant variation took place in the post-lake period as deduced from the analysis of the data collected in that station.

The reason for this apparent contradiction lies in the observational data. Nilo Coelho, the biggest irrigation perimeter in the numerical analyses, was implanted in 1984 and inaugurated in 1989. Nevertheless, most data made available

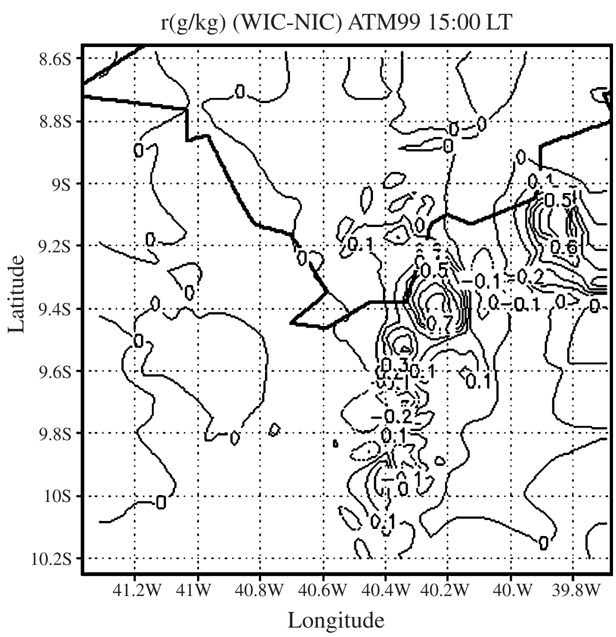

Fig. 11. Mixing ratio ($g\,kg^{-1}$) field at 24 m above the surface at 15:00 LT for ATM99, resulting from the difference between the simulations with irrigated crops (WIC) (without the inclusion of the Nilo Coelho Perimeter) and non-irrigated crops (NIC)

for the statistical analyses were collected during the period 1966–1990 and, consequently do not contain significant information on land use changes in that area. This agricultural area came into full use only in the 1990's. On the other hand, the results obtained by means of observational analyses are compatible with the mixing ratio field as shown in Fig. 11, derived from the difference between the WIC and NIC simulations carried out without the inclusion of the Nilo Coelho Perimeter. It is obvious the absence of the nucleus attributed to Nilo Coelho seen in Fig. 10b.

4. Conclusions

The atmospheric changes that came about after the construction of Sobradinho dam within the semi-arid area of the São Francisco Hydrographic Basin have been assessed by means of the regional model RAMS. A number of numerical experiments were carried out in order to meet several different objectives. To begin with, the construction impact was investigated by considering differences between simulations done with lake (WL) and without lake (NL). On a second stage of the experiments, the influence of the soil occupation on the lake effects was taken into account, considering the lake breeze behavior as the type of vegetation in the surrounding areas of the lake is altered. Finally, considering the development of irrigated areas during the post-lake period, the impacts of changes on soil use brought about by the dam construction was surveyed by means of differences between simulations with (WIC) and without irrigated crops (NIC). The numerical results were compared with statistical data presented in part I of this work.

In assessing the lake impact on the area, one concludes that the model reproduced with accuracy the thermally induced circulations by simulating the well-known attributes of these wind systems.

The lake breeze (LB) varies according to the region's environmental conditions. The intensity of thermally induced circulations can be directly associated with the magnitude and horizontal distribution of the surface heat fluxes. The LB behavior changes with the presence of vegetation in the lake surrounding areas.

In the areas affected by the lake breeze, one can notice a drop in temperature and an increase in air humidity. Such an effect was far stronger in ATM85. The drop in air temperature in the lake area reached up to 3.5 °C and affected a much larger area than that of ATM99. The region that lies east of the 40.5° W meridian, where the meteorological stations of Petrolina, Bebedouro and Mandacaru are located, was not directly affected by the presence of the lake.

In evaluating the impact of changes on soil occupation, the simulations disclosed the presence of an enormous atmospheric sensitivity as to the type of vegetation, being particularly obvious the effect resulting from the inclusion of irrigated crops (IC) on sparsely vegetated areas – most typical of the semi-arid climate, such as the semi-desert type (SD).

Water availability in root zones even under adverse atmospheric conditions (high temperature and low air humidity) is responsible for high evaporation rates and plant transpiration, contributing towards a humidity increase and a temperature fall in the lower atmospheric levels.

The increase in mixing ratio as noticed in simulations of the impact produced by the irrigation perimeters on the Petrolina-Juazeiro axis is in agreement with the results obtained from statistical analyses presented in part I of this work.

One of the main contributions of the present work was to simulate an atmospheric response to changes in land use and soil cover, introducing accurately the location and dimension of the irrigated perimeters as well as the extraction of water by plant roots and its transfer to the atmosphere. By this method one concludes that the statistically significant variations observed in both wind and atmospheric humidity were caused by the changes verified in land use and occupation within the lake region. The replacement of native vegetation by plantations and irrigated crops was rendered responsible for the genesis of a variety of micro-environments in the area under analysis.

Acknowledgement

The authors express their gratitude to the Centro de Pesquisas do Trópico Semiárido/Empresa Brasileira de Pesquisa Agropecuária (CPATSA/EMBRAPA), to the Superintendência do Desenvolvimento do Nordeste (SUDENE), to the Instituto Nacional de Meteorologia (INMET) and to the Companhia Hidrelétrica do São Francisco (CHESF) for providing the data used in Part 1 of this paper. This research was partially supported by the Conselho Nacional de Desenvolvimento Científico e Tecnológico (CNPq).

References

Avissar R, Pan H (2000) Simulations of the summer hydrometeorological process of Lake Kinneret. J Hydrometeorol 1: 95–109

Avissar R, Pielke RA (1989) A parameterization of heterogeneous land surface for atmospheric numerical models and impact on regional meteorology. Mon Wea Rev 117: 2113–2136

Correia AA (2000) Padrões de variabilidade do vento à superfície no Nordeste do Brasil (Patterns of surface wind variability in Northeast Brazil). MSc Dissertation, Universidade Federal da Paraíba, Campina Grande, Brazil

Correia MF, Silva Dias MAF (2003) Variação no nível do reservatório de Sobradinho e seu impacto sobre o clima da região (Variation in the Sobradinho reservoir level and its impact upon the regional climate). Revista Brasileira de Recursos Hídricos 8(1): 157–168

MacCumber MC, Pielke R (1981) Simulation of the effects of surface fluxes of heat and moisture in a mesoscale numerical model. Part I: soil layer. J Geophys Res 86: 9929–9938

Mahrer Y, Pielke RA (1977) A numerical study of the airflow over irregular terrain. Beitr Phys Atmos 50 B: 98–113

Pielke RA (1974) A three-dimensional numerical model of the sea breezes over south Florida. Mon Wea Rev 102: 115–139

Pielke RA, Cotton WR, Walko RL, Tremback CJ, Lyons WA, Grasso LD, Nicholls ME, Moran MD, Wesley DA, Lee TJ, Copeland JH (1992) A comprehensive meteorological modeling system – RAMS. Meteorol Atmos Phys 49: 69–91

Rizzini CT (1997) Tratado de fitogeografia do Brasil (Treatise of phytogeography of Brazil). Âmbito Cultural Edições Ltda.: São Paolo, Brazil

Romariz DA (1996) Aspectos da vegetação do Brasil (Aspects of vegetation of Brazil). Livraria Bio-ciência Ltda.: São Paolo, Brazil

Segal R, Avissar MC, MacCumber R, Pielke A (1988) Evaluation of vegetation effects on the generation and modification of mesoscale circulations. J Atmos Sci 45: 2268–2292

Silva Aragão MR, Correia MF, Sobral ZR (1997) Vento à superfície e chuva em anos contrastantes no submédio São Francisco (Surface wind and rainfall in contrasting years in the lower-middle São Francisco). Boletim Climatológico 2(3): 213–217, Presidente Prudente, Brazil

Silva Aragão MR, Correia MF, Araújo HA (2000) Characteristics of C-band meteorological radar echoes at Petrolina, Northeast Brazil. Int J Climatol 20: 279–298

Tremback CJ, Kessler A (1985) A surface temperature and moisture parameterization for use in mesoscale models. In: Proc. 7th Conf. Numerical Weather Prediction. Amer. Meteor. Soc., Boston, MA, pp 355–358

Tripoli GJ, Cotton WR (1982) The Colorado State University three-dimensional cloud/mesoscale model. Part I: general theoretical framework and sensitivity experiments. J Rech Atmos 16: 186–219

Corresponding author's address: M. F. Correia, Departamento de Ciências Atmosféricas, Universidade Federal de Campina Grande, Aprígio Veloso 882, Bodocongó, CEP 58109-970, Campina Grande, PB (E-mail: magaly@dca.ufcg.edu.br)